Long-term shoreline displacements and coastal morphodynamic pattern of north Rhodes Island, Greece

Gad F.-K.[1], Hatiris G.A.[1,2*], Dimitriadou S.[2], Drakopoulou P.[1,2], Kapsimalis V.[1], Loukaidi V.[1] And Sioulas A.[1]

[1] Hellenic Centre for Marine Research (HCMR), Institute of Oceanography, 46.7 km Athens - Sounio Ave., P.O. Box 712, P.C.19013, Anavissos, Greece

[2] Harokopio University, School of Environment, Geography and Applied Economics, Department of Geography, 70 El. Venizelou Ave., P.C. 17671, Athens, Greece

*e-mail: gahatiris@hcmr.gr

Abstract

An important key element required to develop a reliable and effective Integrated Coastal Zone Management (ICZM) Plan is the in-depth understanding of long-term morphodynamic patterns affecting a coast. The present study investigates the morphological evolution of the north coast of Rhodes Island, Greece resulting from erosion and accretion processes. Long-term shoreline changes were determined from multi-temporal aerial and satellite images (1960-2016) georeferenced and analyzed under a GIS platform (ArcGIS v10.2, ESRI). In addition, the rate-of-change statistics of 24 historic shorelines were calculated using the Digital Shoreline Analysis System (DSAS, USGS). Subsequently, wave and hydrodynamic conditions affecting sediment transport in the coastal area were analyzed by using a dynamic modelling system (MIKE 21/3 Coupled Model FM, DHI). Shoreline displacement occurs mainly at the spit-like northern tip of the study area (Cape of Mylon). This spit-like morphology changes seasonally, due to variations in the annual wave regime. Since 1960, the overall surface area of the backshore has slightly increased with a rate of 36 m^2/y, though in shorter period times large variations has been identified, such as a reduction of 1256 m^2/y between 1960 and 1971 and an increase of 8046 m^2/y between 1990 and 1991.

Keywords: Littoral processes, Sediment transport modelling, GIS analysis

1. Introduction

The coastal zone is a complex system in which complex terrestrial and marine processes interact (Carter, 1988). In such a dynamic system, the description, analysis and interpretation of the involved, natural and anthropogenic, factors are essential for the development of an Integrated Coastal Zone Management (ICZM) Plan. In the context of an ICZM project, Geographic Information Systems (GIS) can provide useful tools for integrating the available spatial data (Clark, 1995, Bartlett and Smith, 2004). For example, a geospatial platform can be applied for historical shoreline mapping, as well as for analyzing shoreline changes and estimating erosion rates. Moreover, numerical modeling is often used for describing and predicting physical processes in the onshore and nearshore environment, over selected space and time scale (Lakhan, 2003). Nowadays, several numerical models are available to simulate coastal hydrodynamic and morphodynamic processes, such as wave propagation, nearshore circulation, sediment transport and shoreline evolution. This study presents the application of both a geospatial platform and a numerical model for the analysis of coastal processes and morphological changes of northern part of Rhodes Island, Greece.

2. The study area

Rhodes Island is located in the Dodecanese insular complex, in the southeastern Aegean Sea, Greece. It is the fourth largest island in Greece, with an area of 1400 km^2 and a coastline length of 253 km. According the 2011 census, the permanent population of the island is 115 490 inhabitants. The case study area is situated on the northern tip of the island, on both sides of Mylon Cape (Figure 1). The length of the coast under investigation is about 1.3 km. The coastline is not straight; in the western part of the area it runs in NE-SW direction with face oriented NW, while in its eastern part is oriented SE-NW facing NE. The beach consists of sand- up to cobble- sized materials (Verikiou-Papaspiridakou *et al.*, 2004, Kombiadou *et al.*, 2009, Anagnostou *et al.*, 2011). The seabed is composed by rock formations and sand and cobble deposits. At depths ranging between 10 m and 30 m, the *Posidonia oceanica* meadow dominates. The data used for the analysis of wind and wave conditions in the study area, have been derived from the “Wind and Wave Atlas of the Hellenic See” (Soukissian *et al.*, 2007). The hind cast data have been generated by numerical models of high spatial and temporal resolution, covering a 10-year period (1995-2004). The prevailing wind directions are west (W) and northwest (NW). However, the strongest winds blow from the southeast (SE), during the winter. As far the wave climate is concerned, the prevailing directions come from the west (W) sector (Figure 1). The strongest wave events propagate from the southeast (SE), occurring mostly during the winter. During strong SE winds with great fetches significant wave height increase up to 4.5 m.

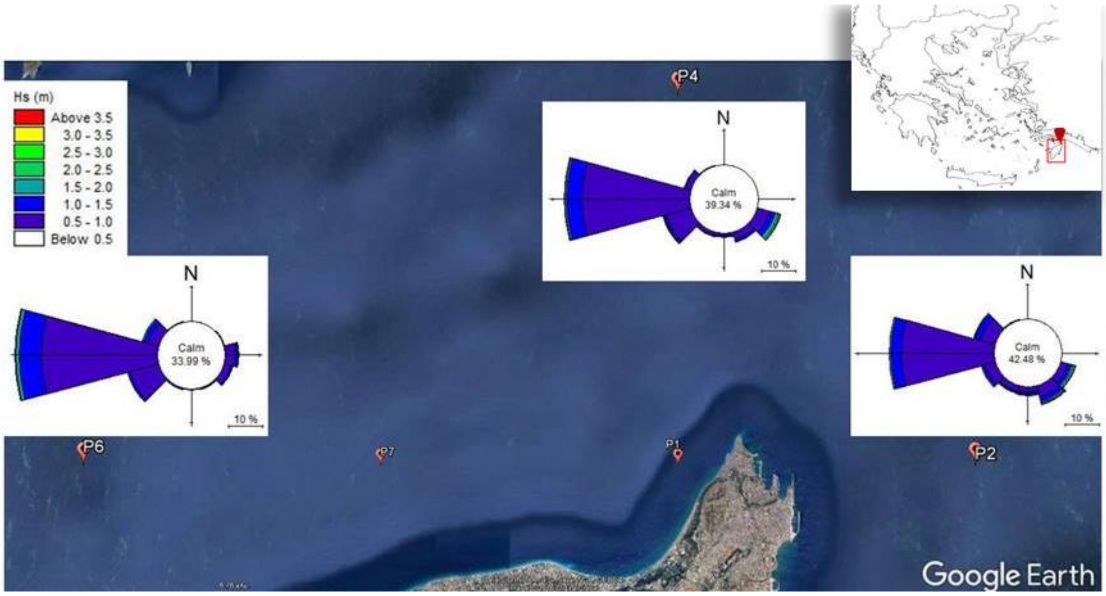

Figure 1. Rose charts offshore Rhodes Island, showing significant wave heights and directions, for the time period 1995-2004.

3. Methodology

Shoreline changes have been determined by using 24 (multi-temporal aerial and satellite) images, which cover the time period 1960-2016. These images were processed with a geospatial platform (ArcGIS, ESRI), while the rate-of-change statistics of the extracted historic shorelines were calculated by means of the Digital Shoreline Analysis System (DSAS, USGS). Subsequently, wave and hydrodynamic conditions affecting littoral drift along the coast were analyzed by using a numerical modelling system (MIKE 21/3 Coupled Model FM, DHI). More specifically, the model was applied to estimate sediment transport, as well as bed level changes. In order to define the shoreline movement within a multi-decade time window at the best possible spatial resolution, 8 black and white aerial photographs covering a 31-year timeline from 1960 to 1991 were obtained in a printed copy form by the Hellenic Military Geographical Service, as well as 16 satellite images covering a 14-year timeline from 2002 to 2016 were downloaded from the Google Earth Pro application. All images were rectified in a GIS environment (ESRI ArcGIS geospatial platform) using as base map the colorful aerial imagery (2007-2009) provided by the National Cadastre and Mapping Agency The selected coordinate system was the WGS 84 (EPSG: 4326) and the projection system was the Greek Grid (EPSG: 2100). Thus, a total of 24 consecutive historical and recent shorelines along the north coast of Rhodes island were delineated / digitized from the rectified multi-dated raster datasets, representing the mean level. Shoreline displacement analysis was performed with the help of the Digital Shoreline Analysis System (DSAS). In particular, the Net Shoreline Movement (NSM) statistical analysis module was used to calculate the displacement distance and rates between the oldest and youngest shoreline in each pair of successive shorelines. For the assessment of sediment transport and coastal morphological changes, a numerical modelling system, namely MIKE 21/3 Coupled Model FM by the DHI, has been used. This model uses a dynamic coupling between spectral wave (SW), hydrodynamic (HD) and sand (non-cohesive sediment) transport (ST) modules, which are some of its computational components. Hence, a feedback of the bed level changes on the wave and current calculations is included (DHI, 2016). The model is based on a flexible mesh approach, giving user the ability to create an appropriate mesh depending on the type of analysis. The model has been applied to four wave scenarios (Table 1) representing annual sediment transport pattern for the study area. The main idea is that the sediment flux is proportional to the energy flux, so a methodology based on wave energy flux has been followed, in order to select simulated scenarios:

- Data are discretized into wave classes with associated annual probability of occurrence. Then, the actual energy flux is estimated as $f_i H_i^2 T_i$, where H_i is the wave significant height, T_i is the wave period and f_i denotes the probability of occurrence of the specific event, i.
- As representative event is defined the one that maximizes the energy flux and its probability of occurrence is determined as

$$f_{max} = \frac{\Sigma\left(f_i H_i^2 T_i\right)}{\left(H_i^2 T_i\right)_{max}} \quad (1)$$

This event causes sediment transport equivalent to the annual budget.

As longshore transport may be to the right (looking seaward) or to the left, depending on wave propagation direction, calculations have been applied to two different groups of events, namely the ones that cause littoral drift to the right and the ones to the left. Bathymetric data were collected during HCMR's Project "AKTI" (Hatiris G.A., 2014) by multibeam survey (Reson Seabat 7125 haul mounted on HCMR's S/V "Alcyone), as well as from maps of the Hellenic Navy Hydrographic Service. Topographic data were acquired from the Hellenic

Table 1. Representative wave scenarios

Scenarios	Hs (m)	Tp (s)	MWD (deg N)	Simulation time (days)
Sc1	1.25	6.75	255	45
Sc2	1.25	5.25	270	39
Sc3	2.25	6.75	135	12
Sc4	1.75	5.25	300	4

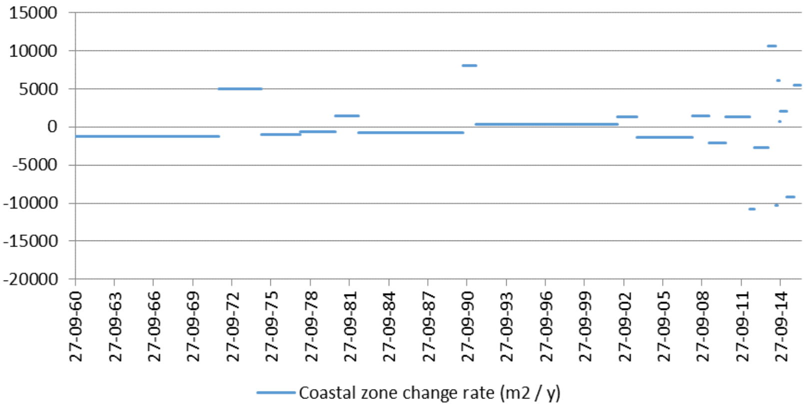

Figure 2. Coastal zone change rates.

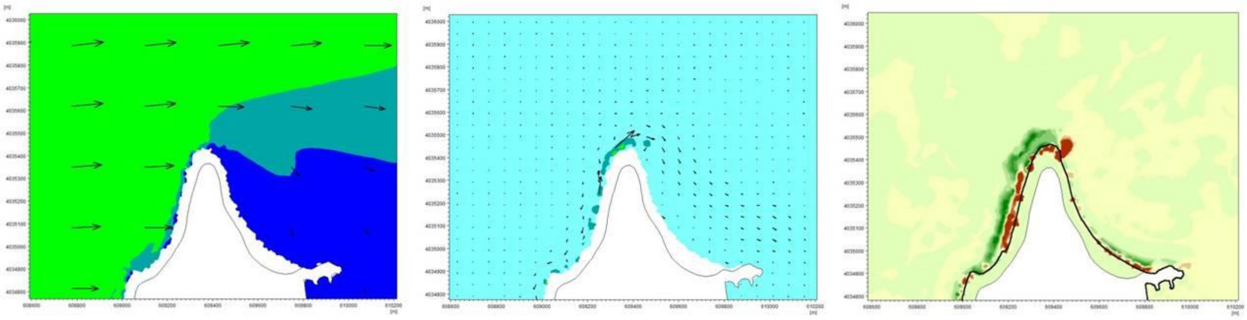

(a) Scenario 1: H_s=1.25 m, T_P=6.75 s, MWD=255 deg N

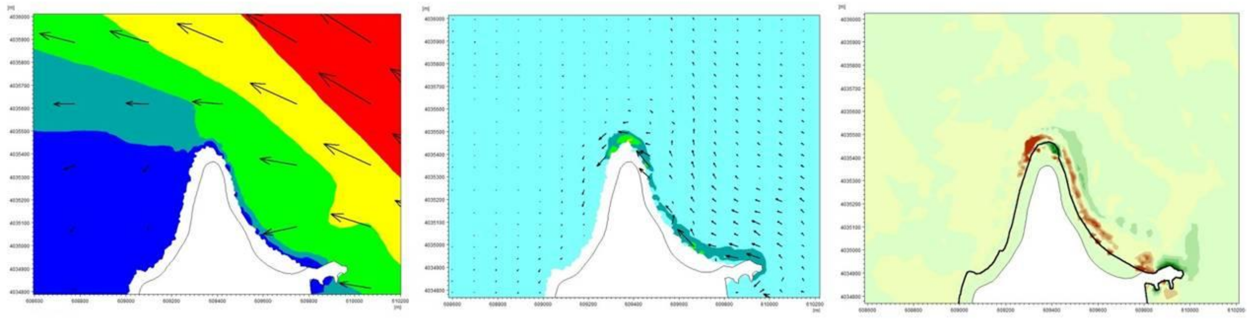

(b) Scenario 3: H_s=2.25 m, T_P=6.75 s, MWD=135 deg N

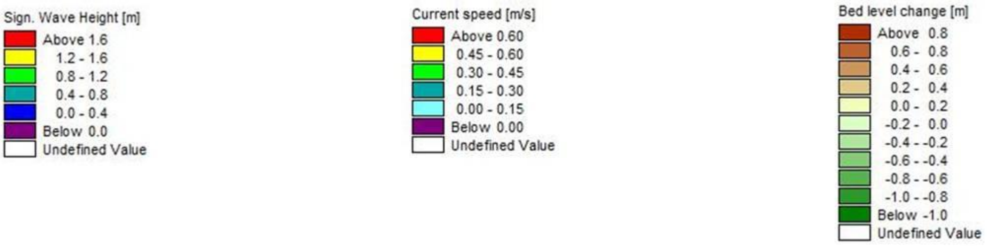

Figure 3. Wave field, current field and bed level change for the modelling of Scenarios 1 (top) and 3 (bottom).

Cadastre. The model domain covers an area of 20 km x 15 km. The mesh consists of 27 777 elements; it is fine in the area of interest and coarse in the rest of the domain. The UTM 35 coordinate system has been specified as reference system in the present study.

4. Results

4.1 Shoreline evolution

Data analysis showed that during the past 56 years the coastal zone of the study area is generally stable, having augmented by almost 2000 m^2, that is augmenting only by almost 36 m^2 per year (Figure 2, Table 2). Nevertheless, both accretion and erosion phenomena are present along the coastal zone of the study area, as the shoreline can advance in some parts of the beach while retreat in others, depending on the beach's orientation against the per season prevailing waves. Shoreline displacement can vary from a few centimeters to several tens of meters. The maximum shoreline advance was measured at 80 m, while the maximum shoreline retreat was found to be around 102 m. The part of the coastal zone most prone to the aforementioned shoreline displacement extremes is unquestionably the spit-like formation at the center of the study area, whose very shape alters from time to time. The western part of the beach is also susceptible to accretion / erosion phenomena, while, on the contrary, the eastern part seems to be more stable. The temporal variability of shoreline position along the coast of the study area appears to be of sub-seasonal timescale, varying even within the time window of a couple of months.

4.2 Morphodynamic pattern

Model results show that prevailing western sector waves (SW, W and NW) induce a northward longshore drift in the western part of the study area, while SE waves result in northward sediment transport in the eastern part of the coast (Figure 3). The latter ones are of high-energy and occur mainly during the winter. Due to these processes sediments are transported and deposited in the northern part of the coast, Cape of Mylon, where a spit is formed. The spit's direction changes gradually, depending on the wave and current conditions, namely it bends east due to western sector waves or west when strong SE wave events occur.

Table 2. DSAS results

Starting shoreline	**Ending Shoreline**	**Max. Advance (m)**	**Min. Advance (m)**	**Max. Retreat (m)**	**Min. Retreat (m)**	**Coastal zone change (m^2)**	**Duration (y)**	**Coastal zone change rate (m^2 / y)**
27-09-60	01-10-71	81	0.03	-56	-0.02	-13835	11.0	-1256
01-10-71	01-01-75	53	0.02	-102	-0.03	16088	3.3	4950
01-01-75	01-01-78	28	0.04	-30	-0.05	-2950	3.0	-983
01-01-78	25-08-80	38	0.14	-24	-0.08	-1763	2.7	-665
25-08-80	15-06-82	28	0.03	-89	-0.01	2568	1.8	1422
15-06-82	20-06-90	77	0.01	-31	-0.01	-5902	8.0	-736
20-06-90	17-06-91	24	0.02	-41	-0.03	7979	1.0	8046
17-06-91	30-03-02	34	0.01	-19	-0.01	3231	10.8	300
30-03-02	12-10-03	41	0.02	-31	-0.01	1962	1.5	1280
12-10-03	01-01-08	41	0.01	-32	-0.01	-5704	4.2	-1352
01-01-08	22-04-09	34	0.01	-98	-0.02	1892	1.3	1446
22-04-09	16-07-10	60	0.02	-25	-0.02	-2546	1.2	-2064
16-07-10	30-05-12	18	0.05	-30	-0.01	2579	1.9	1378
30-05-12	30-09-12	14	0.01	-13	-0.01	-3600	0.3	-10801
30-09-12	09-10-13	12	0.01	-10	-0.01	-2744	1.0	-2677
09-10-13	14-05-14	33	0.01	-57	-0.01	6315	0.6	10573
14-05-14	29-06-14	13	0.01	-16	-0.01	-1282	0.1	-10259
29-06-14	17-08-14	31	0.01	-13	-0.01	815	0.1	6113
17-08-14	02-10-14	15	0.01	-12	-0.02	84	0.1	668
02-10-14	16-03-15	26	0.02	-49	-0.02	3664	0.5	8043
16-03-15	17-10-15	61	0.02	-27	-0.03	-5381	0.6	-9180
17-10-15	21-04-16	13	0.01	-59	-0.02	2809	0.5	5495
21-04-16	27-04-16	13	0.01	-8	-0.02	-953	0.02	-57205
27-09-60	27-04-16	26	0.02	-71	-0.01	2027	55.6	36

5. Conclusion

Since 1960, the overall surface area of the backshore has slightly increased with a rate of 36 m^2/y, though in shorter period times large variations has been identified, such as a reduction of 1256 m^2/y between 1960 and 1971 and an increase of 8046 m^2/y between 1990 and 1991. The model results show that shoreline displacement occurs mainly at the northern tip of the study area (Cape of Mylon), where the sediments are deposited forming a spit. This spit-like morphology changes seasonally, due to variations in the annual wave regime. More specifically, the spit bends east due to western sector waves and it changes direction during the winter, when strong SE wave events occur.

References

Anagnostou C., Antoniou P.F. and Hatiris G.A. (2011), Erosion of a depositional coast in NE Rhodos Island (SE Greece) and assessment of the best available measures for coast protection. Journal of Coastal Research, SI 64 (Proceedings of the 11th International Coastal Symposium), 1316 – 1319.

Bartlett D. and Smith J. (Editors) (2004), GIS for Coastal Zone Management, CRC Press, Boca Raton, FL.

Carter R.W.G. (1988), Coastal Environments - An Introduction to the Physical, Ecological and Cultural Systems of Coastlines, Academic Press Limited, London, UK.

Clark J.R. (1995), Coastal Zone Management Handbook, CRC Press, Boca Raton, FL.

DHI (2016), MIKE 21/3 Coupled Model FM, User Guide.

Hatiris G.A. (2014), INTERREG III GR-CY Project “AKTI”. Technical Report. HCMR, Athens, Greece.

Kombiadou K., Chatiris G.A., Androulidakis I., Sioulas A., Krestenitis Y., Anagnostou C. and Issaris I. (2009), Investigation of erosion at the cape of Rhodos and defence measures, Proceedings of the 9th Symposium on Oceanography and Fisheries, I, 178-183.

Lakhan V.C. (Ed.) (2003), Advances in coastal modeling. Elsevier Oceanography Series, 67, Elsevier, Amsterdam.

Soukissian T., Hatzinaki M., Korres G., Papadopoulos A., Kallos G. and Anadranistakis E. (2007), Wind and wave Atlas of the Hellenic Seas, Hellenic Centre for Marine Res. Publ., Anavissos.

Thieler, E.R., Himmelstoss, E.A., Zichichi, J.L., and Ergul, A. (2009), Digital Shoreline Analysis System (DSAS) version 4.0 — An ArcGIS extension for calculating shoreline change: U.S. Geological Survey Open-File Report 2008-1278. Available online. http://woodshole.er.usgs.gov/project-pages/dsas/

Verikiou-Papaspiridakou E, Bathrellos G. and Skilodikou H. (2004), Physico-geographical observations of the coastal zone of the northeastern part of Island Rhodes, Bulletin of the Geological Society of Greece, XXXVI, 958-967.